Catal Lett (2008) 121:319–323
DOI 10.1007/s10562-007-9341-0

Promoting Role of Fe in the Preferential Oxidation of CO Over Ir/Al_2O_3

Wansheng Zhang · Aiqin Wang · Lin Li · Xiaodong Wang · Tao Zhang

Received: 30 September 2007 / Accepted: 2 November 2007 / Published online: 20 November 2007

Abstract A novel catalyst $Ir–FeO_x/Al_2O_3$ designed for the preferential oxidation (PROX) of CO under excess hydrogen was developed in this work. To clarify the promoting role of Fe species, three different impregnation sequences were employed, and the resultant catalysts were characterized by various techniques. The results showed that the $Ir–FeO_x/Al_2O_3$ catalyst, which was prepared by the co-impregnation procedure, exhibited the best performance for the PROX. The partially exposed and highly dispersed Ir sites and the FeO_x sites allowed good adsorption for both CO and O_2 over the $Ir–FeO_x/Al_2O_3$, which was believed to be responsible for the enhanced activity.

Keywords CO oxidation · PROX · Iron · Iridium · DRIFTS

1 Introduction

Preferential oxidation of carbon monoxide (PROX) in excess hydrogen atmosphere has been regarded as one of the most promising methods, for the removal of CO from H_2-rich gases produced by reforming processes [1, 2]. So far, various catalyst formulations have been investigated for the PROX reaction [3–6], among which supported Pt catalyst was the most intensively studied one. Generally, alumina-supported Pt catalysts behaved actively only at a high temperature, e.g. 150 °C, since O_2 could hardly be adsorbed on the Pt surface covered with strongly adsorbed CO layer at low temperatures. However, at high temperatures, another unexpected reaction of H_2 oxidation became more competitive. Accordingly, to obtain a high activity at low temperatures, in particular at 80 ~ 100 °C, promoters for activating oxygen, such as Fe, Co, Ce, or Sn were employed to form the bimetallic Pt–Fe [7–10], Pt–Co [11], Pt–Ce [12], and Pt–Sn [13, 14] catalysts. Compared with Pt, iridium has received little attention as an active component in the PROX reaction [15]. In this study, we designed a novel catalyst $Ir–FeO_x/Al_2O_3$, and found that this catalyst was very active and selective for the PROX reaction.

W. Zhang · A. Wang · L. Li · X. Wang · T. Zhang (✉)
State Key Laboratory of Catalysis, Dalian Institute of Chemical Physics, CAS, Dalian 116023, P.R. China
e-mail: taozhang@dicp.ac.cn

W. Zhang
Graduate School of the Chinese Academy of Sciences, Beijing 100049, China

2 Experimental

2.1 Catalyst Preparation

The $Ir/FeO_x/Al_2O_3$ was prepared by sequential incipient wetness impregnation. Briefly, γ-Al_2O_3 (S_{BET}: 230 m^2/g) was first impregnated with an aqueous solution of $Fe(NO_3)_3 \cdot 9H_2O$, followed by drying at 85 °C and calcination at 500 °C to obtain FeO_x/Al_2O_3. Then, Ir was deposited on the FeO_x/Al_2O_3 by the same procedure with $H_2IrCl_6 \cdot 6H_2O$ as a precursor. After being calcined at 300 °C for 5 h, the final catalyst $Ir/FeO_x/Al_2O_3$ was obtained. For comparison, a $FeO_x/Ir/Al_2O_3$ catalyst was obtained through an inverse impregnation sequence, while an $Ir–FeO_x/Al_2O_3$ was prepared by co-impregnation method. As reference samples, Ir/Al_2O_3 and Ir/Fe_2O_3 were also prepared by impregnation. The Ir content in all the catalyst samples was fixed at 5wt.%, and the atomic ratio of Fe/Ir was 5/1.

2.2 Catalytic Activity Tests

The catalytic activities were evaluated in a fixed-bed reactor. A reacting gas mixture containing 2% CO, 1% O_2 and 40% H_2 in He was allowed to pass through 100 mg of a catalyst sample at a total flow rate of 67 cm^3/min (STP), corresponding to a space velocity of 40,000 h^{-1}. Prior to the test, the catalyst sample was in-situ reduced with H_2 at 300 °C for 1 h. The effluent gas was analyzed on-line by a gas chromatograph (Angilent GC-6890) equipped with TCD. The conversion and selectivity were defined and calculated as follows:

$$\text{CO conversion } (\%) = \{([\text{CO}]_{\text{in}} - [\text{CO}]_{\text{out}}/[\text{CO}]_{\text{in}}\} \times 100$$

$$\text{O}_2 \text{ conversion } (\%) = \{[\text{O}_2]_{\text{in}} - [\text{O}_2]_{\text{out}}/[\text{O}_2]_{\text{in}}\} \times 100$$

$$\text{CO}_2 \text{ selectivity } (\%) = \{0.5 \times ([\text{CO}]_{\text{in}} - [\text{CO}]_{\text{out}})/([\text{O}]_{\text{in}} - [\text{O}]_{\text{out}})\} \times 100.$$

2.3 Catalyst Characterization

Powder X-ray diffraction (XRD) of the samples was performed on a Rigaku (D/MAX-βB) diffractometer equipped with an on-line computer. Diffraction patterns were recorded with Ni-filtered Cu–Kα radiation (40 kV, 250 mA) over a 2θ range of 10–80°. The high resolution transmission electron microscopy (HRTEM) image was recorded using a Philips CM200 FEG electron microscopy operated at 200 kV. Temperature programmed reduction of hydrogen (H_2-TPR) and chemisorption measurements of CO or O_2 were performed on a Micromeritics AutoChem 2920 apparatus. Prior to the measurement of H_2-TPR, the catalyst sample was pretreated in Ar at 120 °C for 2 h to remove the adsorbed water. After cooling to room temperature in Ar, the gas flow was switched to 10% H_2 in Ar and the sample was heated from room temperature to 800 °C with a temperature ramp of 10 °C/min. The chemisorption measurements were performed at 40 °C after pre-treating the samples in H_2 at 300 °C for 1 h and cooling them to 40 °C in He. In-situ DRIFTS studies were performed using a high pressure DRIFTS cell equipped with CaF_2 windows. Catalyst sample ($\sim$40 mg) in a fine-powder form was placed firmly into the ceramic cup of the DRIFTS cell. All the spectra were collected in a single beam mode, with a resolution of 4 cm^{-1}, using a Bruker EQUINOX 55 Spectrometer equipped with a MCT detector cooled by liquid nitrogen. Before the measurements were taken, the sample was pretreated in 50% H_2/He at 300 °C for 1 h, and then purged in He while being cooled to the desired reaction temperature of 100 °C to allow for the collection of the background spectrum. After that, a reaction mixture containing 2% CO, 1% O_2 and 40% H_2 in He was introduced to the catalyst and the spectrum was recorded under steady state conditions.

3 Results and Discussion

Figure 1 compares the catalytic performances of the Ir/FeO_x/Al_2O_3, Ir–FeO_x/Al_2O_3, FeO_x/Ir/Al_2O_3, Ir/Fe_2O_3 and Ir/Al_2O_3 in the PROX reaction. The Ir/Al_2O_3 exhibited very poor activity, with only less than 10% CO conversion in the temperature range of 60$\sim$150 °C. The Ir/Fe_2O_3 showed a better performance than the Ir/Al_2O_3, with the maximum CO conversion of 47% at 160 °C. In contrast, the Fe-promoted Ir/Al_2O_3 catalysts possessed remarkably enhanced activities. In particular, on the Ir–FeO_x/Al_2O_3 catalyst which was prepared by the co-impregnation, the maximum CO conversion of 74% was obtained at 80 °C. With the difference in the impregnation sequence, the activities varied, following the order of Ir–FeO_x/Al_2O_3 > Ir/FeO_x/Al_2O_3 > FeO_x/Ir/Al_2O_3. On the other hand, the

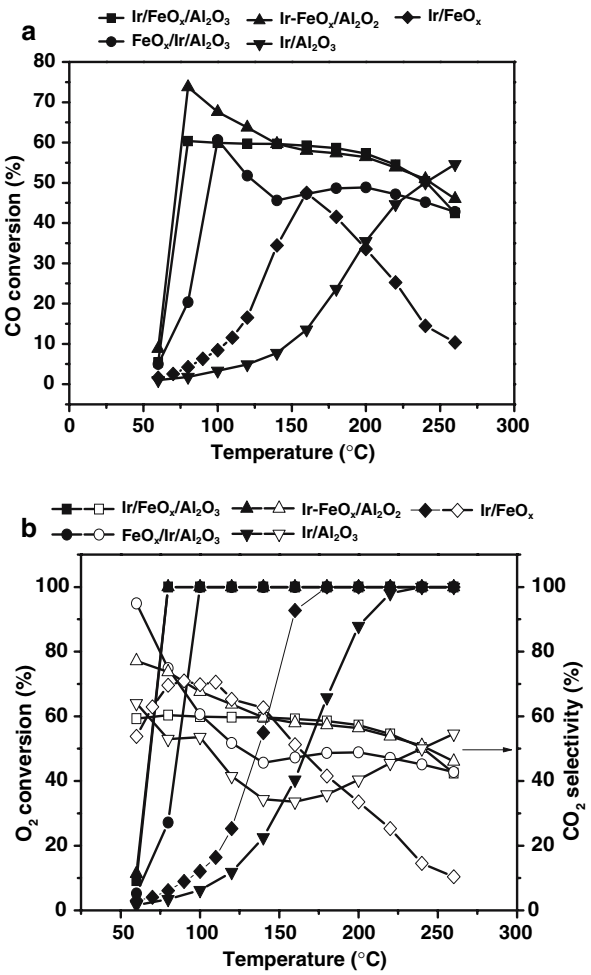

Fig. 1 CO conversions (**a**), O_2 conversions and CO_2 selectivities (**b**) versus reaction temperature over different catalysts

selectivity towards CO conversion was very high over the Ir–FeO_x/Al_2O_3, 74% at 80 °C and it dropped slowly with the reaction temperature rise. The BET surface areas of the above samples (Table 1) are very similar, suggesting the differences in their catalytic activities should not be caused by the variations in the surface areas.

To get the structural information of the different Fe-promoted Ir/Al_2O_3 catalysts, we examined the XRD patterns of the three samples. It should be pointed out that the three samples were pre-reduced by H_2 at 300 °C for 1 h before being subjected to XRD examinations. As shown in Fig. 2, there was no either Ir or FeO_x species which can be detected on the $Ir/FeO_x/Al_2O_3$ and Ir–FeO_x/Al_2O_3 samples, indicating that both Ir and FeO_x are highly dispersed on the alumina support. However, for the $FeO_x/Ir/Al_2O_3$ catalyst, we observed a very weak peak positioned at 41°, which can be attributed to FeO species [JCPDF00-002-1180]. This result suggests that the Ir species is always highly dispersed on the support, irrespective of the impregnation sequence. However, the FeO_x species were better dispersed on the pure alumina support than on the Ir/Al_2O_3 support.

The HRTEM was employed to identify the highly dispersed Ir and FeO_x species on the alumina support. As shown in Fig. 3, the lattice fringes corresponding to γ-Al_2O_3 phase could be observed on the HRTEM image of the Ir–FeO_x/Al_2O_3, while neither iridium nor iron oxide could be identified. However, the EDX analysis showed that both Ir and Fe were present in this region. Therefore, in good agreement with the XRD results, our HRTEM also demonstrated that both Ir and FeO_x were highly dispersed on the Al_2O_3 support.

To clarify the promoting role of the Fe species, H_2-TPR experiments were performed on these catalysts. As shown in Fig. 4, the Ir/Al_2O_3 presents a major reduction peak at around 90 °C and a minor peak centering at 240 °C, which could be ascribed to the reduction of IrO_2 with different sizes [16]. For the FeO_x/Al_2O_3, two broad reduction peaks occurring at 360 °C and 620 °C are observed, which were due to the reduction of Fe^{3+} to Fe^{2+} and further to Fe^0 [17]. In comparison with the Ir/Al_2O_3, the three Fe-promoted

Table 1 The physical properties of different samples and the saturation uptakes of CO and O_2 on the fresh-recuced catalysts (μmol/g-cat)

Catalyst	S_{BET} (m^2/g)	CO adsorption (μmol/g)	O_2 adsorption (μmol/g)	Ir/Fe (atomic ratio, determined by XPS)
FeO_x/Al_2O_3	176	0	150	–
Ir/Al_2O_3	180	77	59	–
$Ir/FeO_x/Al_2O_3$	166	64	396	0.035
Ir–FeO_x/Al_2O_3	198	39	412	0.026
$FeO_x/Ir/Al_2O_3$	181	0	321	0.023

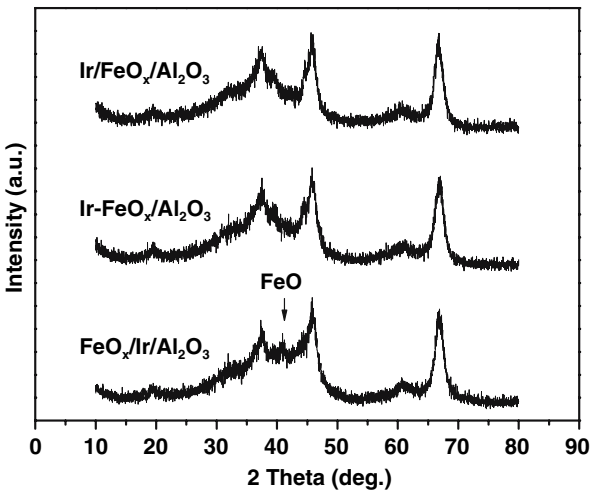

Fig. 2 XRD patterns of $Ir/FeO_x/Al_2O_3$, Ir–FeO_x/Al_2O_3 and $FeO_x/Ir/Al_2O_3$ catalysts which were reduced at 300 °C with H_2

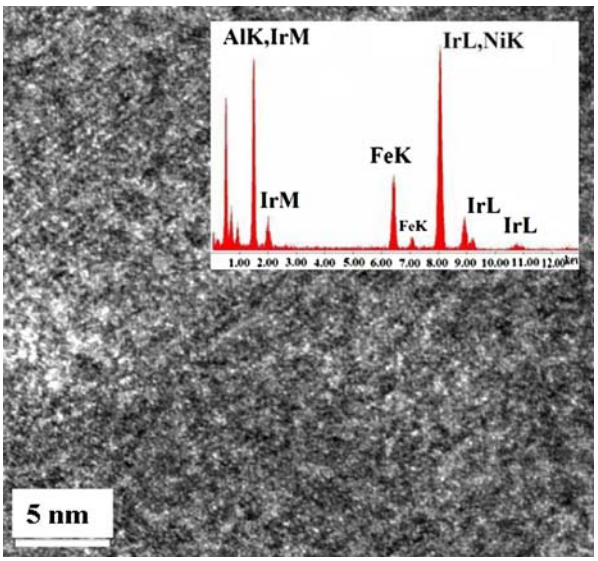

Fig. 3 HRTEM image of the Ir–FeO_x/Al_2O_3 catalyst (inset: EDX spectrum)

Ir/Al_2O_3 catalysts are characterized with a very strong reduction peak at 100 ~ 200 °C, which should be an overlap of the reduction of both Ir^{4+} and Fe^{3+} according to the large consumption amount of H_2. Thus, the reduction of Fe^{3+} could occur at a much lower temperature as a result of hydrogen spillover from Ir to Fe^{3+}, implying a strong interaction between Ir and Fe. Moreover, for the Ir–FeO_x/Al_2O_3 which was prepared by co-impregnation, the first reduction peak appeared at ~150 °C, which was 60 °C lower than that on the $FeO_x/Ir/Al_2O_3$. Since the $FeO_x/Ir/Al_2O_3$ was prepared by the sequential impregnation with first Ir and then Fe, it can be speculated that most of the Ir species were covered by the FeO_x. As a result, its reduction occurred at a higher temperature. On the other hand, the Ir/

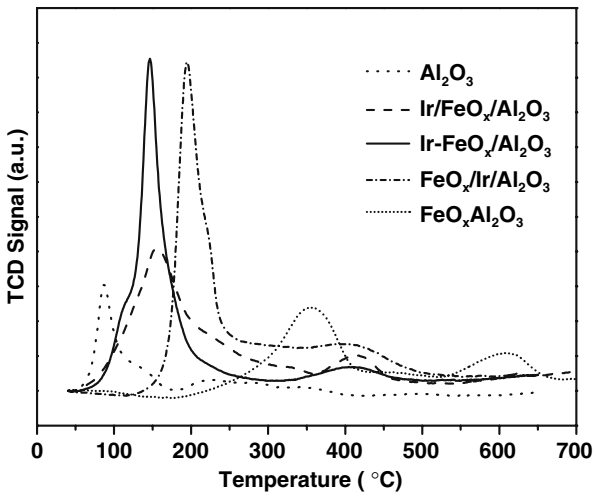

Fig. 4 The H_2-TPR profiles of the calcined catalysts

FeO_x/Al_2O_3 catalyst presented the first reduction peak at only a slightly higher temperature than the Ir–FeO_x/Al_2O_3, but the peak strength of the former was much lower. This result implies that there are more Fe^{3+} ions that could be reduced to Fe^{2+} on the Ir–FeO_x/Al_2O_3 catalyst. Based on the hydrogen consumption, it could be roughly estimated that the percentage of the reducible Fe^{3+} ions on the Ir/FeO_x/Al_2O_3, Ir–FeO_x/Al_2O_3 and FeO_x/Ir/Al_2O_3 was 23%, 53% and 55%, respectively. Correlating with the catalytic performance, it can be seen that the reduction behavior, especially the first reduction peak temperature, is coherent with the activity level.

The catalyst structure was further uncovered by the in-situ DRIFTS. The pre-treatment condition was the same with the activity test, and the reaction temperature was fixed at 100 °C. As shown in Fig. 5, The Ir/Al_2O_3 presented two absorption bands at 2060 and 1970 cm^{-1},

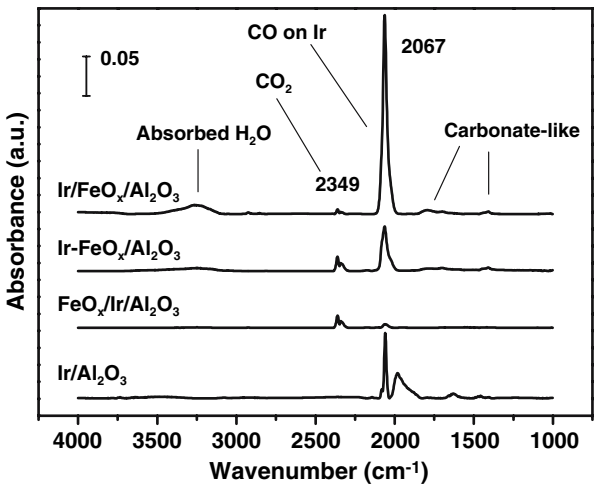

Fig. 5 In-situ DRIFTS spectra on the fresh-reduced catalysts under PROX condition (catalyst weight: 40 mg; total flow: 100 mL/min)

which should be assigned to the linear and bridged CO adsorption on Ir sites [18]. No CO_2 gas peak was observed on the Ir/Al_2O_3 during the PROX reaction. Compared with the Ir/Al_2O_3, a strong linearly adsorbed CO band at 2067 cm^{-1} appeared on the $Ir/FeO_x/Al_2O_3$. It is noted that the intensity of this band differed markedly on the three catalysts, following the order of $FeO_x/Ir/Al_2O_3$ < Ir–FeO_x/Al_2O_3 < $Ir/FeO_x/Al_2O_3$. This result indicates that the exposed Ir sites on the $Ir/FeO_x/Al_2O_3$ are the most while those on the $FeO_x/Ir/Al_2O_3$ are the least. This result was further confirmed by our XPS analysis. As shown in Table 1, the surface Ir/Fe atomic ratio on the $Ir/FeO_x/Al_2O_3$, Ir–FeO_x/Al_2O_3, $FeO_x/Ir/Al_2O_3$ catalysts was 0.035, 0.026 and 0.023, respectively. Since the bulk Ir/Fe ratio on the three samples was 0.2, the unexpected low surface Ir/Fe ratio suggests a significant enrichment of Fe on the catalyst surface. In addition to the CO adsorption band, the band at 2349 cm^{-1} can be attributed to the gas phase CO_2, while the bands between 1800 ~ 1000 cm^{-1} are assigned to the carbonate-like species. A broad band at 3300 cm^{-1} appeared on the $Ir/FeO_x/Al_2O_3$ and Ir–FeO_x/Al_2O_3 catalysts, which can be attributed to the adsorbed H_2O coming from the oxidation of H_2 in the PROX reaction. In agreement with the activity test results, the intensity of the CO_2 band on the Ir–FeO_x/Al_2O_3 is the strongest. The above result seems to suggest that the Ir–FeO_x/Al_2O_3 catalyst, with a part of Ir sites exposed on the surface while another part covered by the FeO_x species, should provide sites for both CO adsorption and O_2 activation.

To corroborate this, the chemisorption of CO and O_2 was performed, and the saturation uptakes are listed in Table 1. Clearly, the FeO_x/Al_2O_3 could not adsorb CO at all. Similarly, the $FeO_x/Ir/Al_2O_3$ had only a negligible adsorption amount of CO, indicating most of the Ir species in this catalyst was covered by the FeO_x. In contrast, a significant amount of CO could be adsorbed on the Ir–FeO_x/Al_2O_3. Moreover, the CO uptake on the Ir–FeO_x/Al_2O_3 was 39 μmoL/g while it was 64 μmoL/g on the Ir/FeO_x/Al_2O_3 catalyst, implying that less Ir sites were available on the Ir–FeO_x/Al_2O_3 catalyst. Compared with the Ir/Al_2O_3, the $Ir/FeO_x/Al_2O_3$ adsorbed only a slightly lower amount of CO. Considering that the deposition of FeO_x on the Al_2O_3 would lead to a slight decrease in the specific surface area (Table 1), we believe that in the Ir/FeO_x/Al_2O_3 catalyst, most of the Ir species were exposed on the surface, just like the case of the Ir/Al_2O_3. On the other hand, for the O_2 adsorption, the three Fe-promoted Ir/Al_2O_3 catalysts exhibited much higher O_2 uptakes, as compared to the Ir/Al_2O_3. Clearly, the role of FeO_x was mainly to adsorb and activate O_2. In particular, the Ir–FeO_x/Al_2O_3 exhibited the highest O_2 uptake, which should be attributed to the adsorption of O_2 on both the Ir sites and on the FeO_x sites. The above results showed that

the activation of O_2 was improved greatly while the CO adsorption could still occur on the most active Ir–FeO_x/Al_2O_3 catalyst.

In summary, we have developed a very active and selective catalyst Ir–FeO_x/Al_2O_3 for the PROX reaction. On this catalyst, the exposed Ir acted as the adsorption sites for CO while the FeO_x played the major role in the activation of oxygen. By this way, a non-competitive L–H reaction pathway was established and the catalytic performance was improved significantly.

Acknowledgments Support of National Science Foundation of China (NSFC) for Distinguished Young Scholars (No. 20325620) is gratefully acknowledged.

References

1. Choudhary TV, Goodman DW (2002) Catal Today 77:65
2. Dudfield CD, Chen R, Adcock PL (2000) J Power Sources 86:214
3. Trimm DL, Onsan ZI (2001) Catal Rev 43:31
4. Trimm DL (2005) Appl Catal A 296:1
5. Kim WB, Voitl T, Rodriguez-Rivera GJ, Evans ST, Dumesic JA (2005) Angew Chem Int Ed 44:778
6. Grisel RJH, Nieuwenhuys BE (2001) J Catal 199:48
7. Sirijaruphan A, Goodwin JG Jr, Rice RW (2004) J Catal 224:304
8. Watanabe M, Uchida H, Ohkubo K, Igarashi H (2003) Appl Catal B 46:595
9. Kotobuki M, Watanabe A, Uchida H, Yamashita H, Watanabe M (2005) J Catal 236:262
10. Liu XS, Korotkikh O, Farrauto R (2002) Appl Catal A 226:293
11. Kwak C, Park TJ, Suh DJ (2005) Appl Catal A 278:181
12. Özkara S, Aksoylu AE (2003) Appl Catal A 251:75
13. Simsek E, Özkara S, Aksoylu AE, Önsan ZI (2007) Appl Catal A 316:169
14. Schubert MM, Kahlich MJ, Feldmeyer G, Huttner M, Hackenberg S, Gasteiger HA, Behm RJ (2001) Phys Chem Chem Phys 3:1123
15. Mariño F, Descorme C, Duprez D (2004) Appl Catal B 54:59
16. Carnevillier C, Epron F, Marecot P (2004) Appl Catal A 275:25
17. Wan HJ, Wu BS, An X, Li TZ, Tao ZC, Xiang HW, Li YW (2007) J Nat Gas Chem 16:130
18. Solymosi F, Novak E, Molnar A (1990) J Phys Chem 94:7250